Generation of mechanosensory neurons in adult *Drosophila*

Authors: Ismael Fernández-Hernández[1], Evan B. Marsh[1], Michael A. Bonaguidi[1,2].

Affiliations:

[1] Department of Stem Cell Biology and Regenerative Medicine, Eli and Edythe Broad Center for Regenerative Medicine and Stem Cell Research, Keck School of Medicine; [2]Department of Biomedical Engineering, Center for Neural Engineering, Viterbi School of Engineering; Department of Gerontology; Zilkha Neurogenetic Institute, University of Southern California; Los Angeles, CA, 90033; USA

SUMMARY

Auditory and vestibular mechanosensory hair cells in the adult mammalian inner ear do not regenerate following injury or ageing, inducing irreversible hearing loss and balance disorders for millions of people. Research on model systems showing replacement of mechanosensory cells can provide mechanistic insight to develop new regenerative therapies. Here we developed new lineage tracing systems to reveal the generation of mechanosensory neurons (Johnston's Organ, JO) in the antennae of intact adult *Drosophila*. New JO neurons develop cilia, express an essential mechano-transducer gene and target central brain circuitry. Furthermore, we identified low-level JO self-replication as a new mechanism of neuronal plasticity. Overall, our findings introduce a new platform to expedite the research of mechanisms and compounds mediating mechanosensory cell regeneration.

INTRODUCTION

Hearing and balance disorders affect over 5% of the world's population, with 1 in 3 people affected by the age of 80, and 900 million expected by 2050 (Geleoc and Holt, 2014 , WHO 2019). This is due to the degeneration of mechanosensory hair-cells and their innervating neurons in the inner ear following damage by genetic mutations, excessive noise, ototoxic drugs or ageing. Unfortunately, no treatments exist to replenish lost cells in the human sensory epithelia (Müller and Barr-Gillespie, 2015). Thus, regenerative strategies are urgently needed to recover auditory and vestibular function for millions of people. While non-mammalian vertebrates are able to functionally replenish hair-cells throughout life (Kniss et al., 2016; Ryals et al., 2013; Stone and Cotanche, 2007), mammals show scarce regenerative capacity at early postnatal stages in the cochlea (Bramhall et al., 2014; Cox et al., 2014; Kelley et al., 1995; White et al., 2006) and very low levels in adult vestibular organs (Bucks et al., 2017; Forge et al., 1993; Golub et al., 2012; Kawamoto et al., 2009; Warchol et

al., 1993). In all cases,non-sensory supporting cells trans-differentiate to regenerate hair cells (Atkinson et al., 2015; Bucks et al., 2017; Kniss et al., 2016; Stone and Cotanche, 2007; White et al., 2006). Still, research on these models at genetic, cellular, circuitry and behavioral levels is costly and technically challenging.

The fruit fly *Drosophila melanogaster* harbors ciliated mechanosensory neurons known as Johnston's Organ (JO) on the second segment of its two antennae. JO are clustered in ~200 scolopidia per antenna, comprising multicellular units with 2-3 JO neurons and surrounding supporting cells (Boekhoff-Falk and Eberl, 2014)(Albert and Go, 2015)(Ishikawa and Kamikouchi, 2016). JO develops under conserved genetic programs with and act as counterparts to mammalian hair-cells and their innervating neurons, by supporting auditory and vestibular functions (Boekhoff-Falk, 2005; Eberl and Boekhoff-Falk, 2007; Kamikouchi et al., 2009; Li et al., 2018; Sun et al., 2009; Wang et al., 2002). *Drosophila* represents a compelling platform to accelerate research on functional regeneration of mechanosensory cells due to genome-wide available due to unparalleled available genetic tools, a detailed characterization of JO neurons at the circuitry- and behavioral-level (Ishikawa et al., 2017; Kamikouchi et al., 2006; Lai et al., 2012; Matsuo et al., 2016; Vaughan et al., 2014) and simple scalability at low cost. Yet, turnover of JO neurons has not been reported thus far. Since adult neurogenesis occurs in certain regions of the *Drosophila* brain (Fernández-Hernández et al., 2013), we hypothesized the peripheral nervous system also contains this capacity. We implemented a modified lineage tracing system which revealed adult-born JO neurons by live imaging on intact adult *Drosophila*. New JO acquire features of mature, functional neurons. Furthermore, we captured low-frequency JO self-renewal as a new mechanism to counteract neuronal cell death. Our results provide a new *in vivo* platform to screen for compounds promoting mechanosensory cell regeneration, their mechanisms of action and functional outcomes at circuitry and behavioral level.

RESULTS

P-MARCM detects adult neurogenesis in Drosophila brain

In order to detect low levels of cell proliferation in adult *Drosophila* in a cell type-specific and sustained manner, we developed P-MARCM (Permanent-MARCM). Built upon MARCM (Lee and Luo, 1999), P-MARCM becomes permanently active upon heat shock to detect sporadic mitotic events in virtually any adult tissue and label specific cell populations generated. Briefly, a heat shock-induced pulse of Flippase (Flp) excises an FRT-flanked STOP codon between *tubuline* promoter and *lexA* transactivator (Singh et al., 2013), which in turn binds to *lexAOp-Flp* sequence (Pfeiffer et al., 2010) to drive Flippase permanently in heat shock-responding cells (Figure 1A,B). Specificity for cell-labeling is achieved by incorporation of desired *GAL4* lines, to express nuclearly-

localized RFP (Barolo et al., 2004) and membrane-tagged GFP (Shearin et al., 2014) only in adult-born cells of interest in the lineage. This allows for cell quantification and morphology assessment concurrently (Figure 1C). As validation, P-MARCM detected previously reported neurogenesis in the adult optic lobes (Fernández-Hernández et al., 2013) by using the pan-neuronal *nsyb-GAL4* line (figure supplement 1). Thus, P-MARCM serves as an entry point to capture adult-cell proliferation in a cell type-specific manner.

Identification of JO neurogenesis by P-MARCM

In order to assess the generation of JO neurons in adult *Drosophila*, we used P-MARCM containing *iav-GAL4* line (Kwon et al., 2010)(Ishikawa et al., 2017). *iav* (inactive) is a transient receptor potential (TRP) vanilloid channel expressed exclusively in the cilia of chordotonal neurons, and is essential for mechano-transduction in hearing (Gong et al., 2004). Importantly, incorporation of enhanced nuclear-RFP (Barolo et al., 2004) and membrane-GFP (Shearin et al., 2014) reporters in P-MARCM permits direct identification of JO neurons by live imaging on intact flies (Figure 1D). We therefore activated P-MARCM *iav-GAL4* adult flies and conducted single-fly time-lapse imaging over 4 weeks (Figure 1E). Remarkably, this approach revealed JO neuron generation in P-MARCM flies (47%, n=19 flies), at a higher frequency and extent than transient, regular MARCM (15%, n=20 flies) (Figure 1F-G).

We then quantified JO neurogenesis by confocal imaging on P-MARCM *iav-GAL4* dissected antennae over 4 weeks (Figure 2A). While MARCM detected minimal to no-neurogenesis, P-MARCM captured JO neurogenesis at different extents over time, with 11-38 JO neurons/fly across time points (avg. 20.2 +/-7.3SD neurons/fly) (Figure 2 B-D, figure supplement 2A). Clustering flies into 'Responders'/'Non-responders' (*i.e.* JO neurogenesis present/absent) by a Gaussian mixture model (figure supplement 2B; see methods) revealed a significant increase in the number of 'Responders' over time (Figure 2E), including 57% by 4 weeks and 42% across time points. This outcome is consistent with the 47% ratio detected by our previous live imaging approach (Figure 1G). Altogether, our results identify JO neurogenesis in adult *Drosophila* using complementary *in vivo* time-lapse imaging and confocal microscopy approaches.

Adult-born JO neurons mature and target brain circuitry

We next evaluated the cellular features of newborn JO neurons. We imaged antennae and brains of P-MARCM *iav-GAL4* flies with JO neurogenesis detected after 4 weeks (Figure 3A) (representative images shown for fly in Figure 1F). At the cellular level, adult-born JO neurons develop cilia, express the essential mechano-

transducer channel *iav* (Gong et al., 2004) and extend axons (Figure 3B). At the circuit level, new JO target the brain through the Antennal Mechanosensory and Motor Center (AMMC) in the auditory and vestibular pattern (Figure 3C), inferred from their axonal projections to the brain (Ishikawa and Kamikouchi, 2016; Kamikouchi et al., 2006) (Figure 3C). These features were consistently found in all the cases analyzed. Altogether, these observations strongly suggest the ability for new JO neurons to mature and functionally remodel the mechanosensory circuitry.

Self-replication of JO neurons

Since P-MARCM becomes randomly activated by heat shock in different cell types (Figure 1A,B), we next sought to identify a cellular source for adult-born JO neurons. In vertebrates, hair cell regeneration involves trans-differentiation of non-sensory supporting cells (Atkinson et al., 2015; Brignull et al., 2009). Recent studies demonstrate 'tailored' mechanisms for cell replacement including proliferation of undifferentiated progenitors, de-differentiation and division of mature cells, and direct mitosis of post-mitotic cell types (Post and Clevers, 2019). We therefore considered three possible sources of adult JO neurons: 1) undifferentiated progenitors from development; 2) non-sensory supporting cells in the scolopidium; and 3) pre-existing JO neurons. The first two options would require high levels of architecture remodeling to develop entirely new scolopidia or incorporate new JO inside the tightly-packed existing units. Instead, self-renewal of JO neurons would facilitate proper incorporation, anchoring and targeting of new neurons into the scolopidium and the brain circuitry. In support of this hypothesis, a detailed analysis of P-MARCM-*iav* and MARCM-iav confocal images revealed instances of JO resembling self-division (1.3%, n=557 neurons analyzed), such as split DNA and pairs of labeled JO with intermingled cilia and axons (Figure 4A-C).

In order to confirm mitotic activity in JO neurons, we implemented a JO-driven lineage tracing method. Here, *iav*+ JO neurons constitutively express the recombinase Flippase and a single copy of UAS-GFP reporter, distal to an FRT site on second chromosome. Upon mitosis, one daughter JO becomes homozygous for GFP, clearly distinguishable from the single-copy GFP background by live imaging (Figure 4D). Remarkably, this approach captured low-level JO self-renewal at different points over 4 weeks in 21% of the flies analyzed (n=72 flies, 1-11 cells/antenna) (Figure 4E-F). Importantly, JO self-renewal was detected in males and females at similar frequencies (53% males, 47% females, n=15 flies), and in some cases with single-neuron resolution (Figure supplement 3). Further, we identified 2xGFP JO-axon bundles in the brain, indicating JO replication from cell bodies to terminal connections (Figure 4G). Importantly, this system marks only half of the new JO neurons

remaining upon mitosis and therefore underrepresents the amount of JO self-renewal. We ensured that neurons labeled appeared in adult stages by first removing any 'escapers' labeled by leaky expression of Flippase during development, which occurs at very low rates (2.3%, n=306 flies assessed). Our results uncover an unexpected potential in *Drosophila* neurons to self-divide as a new mechanism for nervous system regeneration.

JO cell-turnover

We finally asked whether JO regeneration occurs as an additive or cell turnover mechanism within mechanosensory circuitry. Immunostaining for cleaved-Caspase3 (Ca3) revealed JO apoptosis at a higher frequency and extent in posterior (5.8+/-1.0(sem) Ca3+ neurons/antenna, 100% antennae, n=33) compared to anterior neurons (1.5+/-0.25 Ca3+ cells/antenna, 12% antennae, n=33) (Figure 5A, C-D). Accordingly, P-MARCM captured JO neurogenesis at higher frequency and extent on posterior (8.7+/-2.2 neurons/antenna, 69% antennae, n=16) than anterior regions of the antenna (2.4+/-1.0 neurons/antenna, 44% antennae, n=16) (Figure 5B-D). These correlations strongly suggest JO cell-turnover. Supporting this finding, JO self-renewal was also detected by JO-specific lineage tracing system in the vicinity of apoptotic cells (Figure 5D). Taken together, these results describe cellular plasticity in the mechanosensory system of adult *Drosophila*, pointing to a cell-turnover mechanism to potentially preserve auditory and vestibular functions.

DISCUSSION

Development of regenerative interventions for lost hair-cells are urgently needed. However, the field has been hampered by the lack of *in vivo,* high-throughput platforms to easily assess adult functional regeneration of sensory cells at the genetic, neural circuitry and behavioral level. To this aim, we developed P-MARCM -a modified lineage tracing system in *Drosophila* to capture cell-type-specific proliferation in adult tissues over time without immunostaining. P-MARCM successfully detected previously reported low-rate neurogenesis and regeneration in adult optic lobes (Fernández-Hernández et al., 2013). We leveraged the versatility of P-MARCM to identify adult genesis of JO neurons, the functional counterparts to vertebrate hair-cells, by time-lapse imaging of intact flies and confocal microscopy. Therefore, addition of new cells can be witnessed in external organs *in vivo* over time, allowing for tracking of cell proliferation at the single-fly level. Furthermore, incorporation of an additional *UAS*-construct allows genetic manipulation of adult-born cells to assess their functional contribution. For example, JO neurons contribution to auditory and vestibular function could be assessed in future experiments, by applying existing behavioral protocols (Inagaki et al., 2010; Kamikouchi et

al., 2009; Vaughan et al., 2014). Indeed, our results suggest new JO neurons have the potential to functionally modify mechanosensory circuitry, since they develop sensory cilia, express an essential mechano-transducer gene and target the brain. This system will also allow research on mechanisms driving synapsis formation between new and pre-existing neurons.

We focused on identifying a cell-of-origin for new JO neurons. Analysis of P-MARCM images prompted us to hypothesize JO neurons could self-divide and remain in the tissue. Surprisingly, we identified low-level JO self-replication by live imaging using an independent JO-specific lineage tracing method. These results revealed an unexpected proliferative capacity in JO neurons and confirmed P-MARCM observations. We suggest JO self-renewal can occur in Drosophila because i) JO neurons are enclosed by three distinct supporting cells in the scolopidia, making external incorporation of JO challenging; ii) each scolopidia contains 2-3 JO neurons, which can constitute a back-up mechanism to promptly replace lost JO without compromising other scolopidial cell types; and iii) self-division would facilitate proper cilia- and axon-targeting for optimal function in new JO.

We detected low-levels of JO apoptosis spatially correlated with JO neurogenesis, suggesting cell-turnover (Figure 5). A similar low-turnover of vestibular hair-cells occurs in vertebrates (Bucks et al., 2017; Kil et al., 1997), which increases following acoustic- or chemical-injury (Bucks et al., 2017; Corwin and Cotanche, 1988; Ryals and Rubel, 1988; Williams and Holder, 2000). Therefore, the cell-turnover of JO neurons in *Drosophila* suggests they may retain the potential for repair upon different forms of injury.

The differences in JO neurogenesis detected by JO-specific lineage tracing (21% of flies) compared to P-MARCM (45% of flies) suggests either other cell types (undifferentiated- or supporting-cells activated in P-MARCM) might still act as progenitors, or different recombination efficiencies could exist between methods. Nevertheless, self-renewal of sensory cells represents an unexpected mechanism to be further investigated in sensory cells regeneration.

Recent efforts have established mammalian *in vitro* platforms for drug screenings to promote hair-cells renewal (Costa et al., 2015; Koehler et al., 2017, 2013; Landegger et al., 2017). Although useful, these platforms lack physiologic environment and systemic cues, such as those controlling tissue interactions and drug metabolism and availability. In our case, the low-levels of JO self-division and the sensitivity to resolve single-neurons by time-lapse imaging on individual flies provides an *in vivo* scalable platform to screen for small-molecules that enhance JO regeneration (Fernández-Hernández et al., 2016). For selected targets, the transcriptomic and epigenetic changes on JO neurons can be assessed as they occur *in vivo*, by genetically-encoded available tools (Marshall et al., 2016; Marshall and Brand, 2017; Southall et al., 2013). Further,

functional contribution of regenerated JO can be readily assessed by established behavioral protocols (Kamikouchi et al., 2009; Sun et al., 2009; Vaughan et al., 2014). Altogether, the new *Drosophila* platform presented here represents a promising approach to identify modifiers of neuronal regeneration, their mechanisms of action and the functional consequences at circuitry and behavioral levels.

METHODS

Fly stocks

For P-MARCM-iav and MARCM-iav experiments.

Female virgins of genotype *hs-Flp,tub-GAL80,neoFRT19A ; hs-FlpD5,20UAS-6GFPmyr,UAS-RedStinger / CyO ; iav-GAL4* were crossed to males of genotype *tub FRT STOP FRT lexA,neoFRT19A ; + ; 8lexAOp-Flp/TM6B*. The cross was set and kept at 17C during development to minimize spontaneous *hs-Flp* activation. For P-MARCM, 2-5 days old female virgins were picked with final genotype: *hs-Flp,tub-GAL80,neoFRT19A / tub FRT STOP FRT lexA,neoFRT19A ; hs-FlpD5,20UAS-6GFPmyr,UAS-RedStinger / + ; iav-GAL4 / 8lexAOp-Flp*. For MARCM, females of same age and genotype, but carrying a *TM6B* balancer chromosome instead of *8lexAOp-Flp* were picked. *hs-FlpD5* was inserted to maximize Flp induction and recombination. Every single fly of these genotypes was then pre-screened under epi-fluorescent scope to ensure only those with minimum- to no-background labelling were taken for proliferation analysis. Selected flies were then pooled and some of them randomly picked for dissection as controls. Remaining flies were allocated for activation by heat shock and dissection at later time points. In order to maximize the number of cells were the system gets activated, we heat shocked flies at 38C (Ohlstein and Spradling, 2006) for 30 minutes twice on the same day, ~2 hours apart.

For JO-driven (iav-GAL4) lineage tracing system

Female virgins of genotype *w ; UAS-CD8-GFP,UAS-CD2mir,FRT40A ; 20UAS-FlpD5* were crossed to males *w; tubQS,FRT40A ; iav-GAL4.* Males and females 2-5 days old of final genotype *w ; UAS-CD8-GFP,UAS-CD2mir,FRT40A / tub-QS,FRT40A ; 20UAS-FlpD5 / iav-GAL4* were picked and screened individually by fluorescent microscopy to remove those with background labeling. Selected flies were tracked over time and imaged by time lapse imaging (see below). Those with neurogenesis were harvested and processed for confocal imaging as described below.

Dissection and immunostaining. Antennae were dissected, attached to their corresponding brains in chilled Schneider's medium and then fixed in 3.7% formaldehyde solution for 20 min. They were then washed with PBT 1% solution for 10-20 min, followed by a final wash in 1XPBS before incubation with primary antibodies overnight at 4C (2 nights for nc-82 antibody), followed by incubation with secondary antibody 4 hours at room temperature or overnight at 4C. For staining of neurons and caspase third segment of antennae was removed before fixation, to facilitate antibody penetration to JO neurons. Primary antibodies used: mouse anti-nc82 (1:10, DSHB), rat anti-elav (1:100, DSHB), rabbit anti-cleavedCaspase3 (1:200, Cell Signaling); secondary antibodies (Jackson laboratories): anti-mouse Cy5 antibody (1:100), anti-rat Cy5 (1:100), anti-rabbit Cy3 (1:200). No antibodies were used for GFP and RedStinger fluorescent proteins. Antennae and brains were mounted in Vectashiled media with DAPI (Vector laboratories). For mounting, we used double-side sticker spacers (EMS, 70327-9S) to preserve morphology as much as possible. We use one spacer for antennae and two for matching brains.

Time lapse imaging of live flies. Flies were anesthetized on a CO2 pad for imaging under a Zeiss V16 epi-fluorescent scope with a 5.6Mp monochrome camera. These acquisition settings were selected to image P-MARCM flies in order to preserve viability after imaging over time: 50% power lamp, PlanApo 1X objective, 85% aperture, 160X total magnification, 5x5 camera binning, 90ms exposure time for GFP and RFP channels and, on average a ~100 um Z-stack with 4um increments. For JO-lineage tracing 4x4 camera binning and 25ms exposure time for RFP were selected. Maximum intensity projections were generated for display.

Gaussian mixture model method. Labeled neurons were counted in JO of each fly, from across all time points. Assuming JO from any time point fell into either "Responder" or "Non-Responder" categories, we fit a Gaussian mixture model with two mixture components using the mclust package (Scrucca et al., 2016) with default parameters. The model found that any fly with 9 or fewer neurons was in the 'Non-Responder' category (*i.e.* comparable to system background levels), accounted for 63% of all observations, while any fly with 10 or more neurons was a 'Responder', (*i.e.* above background levels) accounted for the remaining 37%.

Acknowledgements

We thank members of the Bonaguidi lab for support, specially Maxwell Bay for assistance with Gaussian model and statistical analysis and Eric Hu for technical assistance with maintenance of fly lines; Dr. Neil Segil (USC) for insightful discussions on this project; Dr. Matthias Landgraf (U. Cambridge) for kindly providing *tub>STOP>lexA* flies; Bloomington Drosophila Stock Center (NIH P40OD018537) for other lines used in this

study; Developmental Studies Hybridoma Bank, created by the NICHD of the NIH for nc-82 and elav antibodies. Authors acknowledge support from USC-CONACYT Postdoctoral Scholars Program Fellowship and USC Provost's Postdoctoral Scholar Research Grant to I.F.-H.; USC Provost Undergraduate Research Fellowship to E.B.M. and NIH (R00NS089013, R56AG064077), Whittier Foundation and Baxter Foundation to M.A.B.

REFERENCES

Albert T, Go MC. 2015. Hearing in Drosophila. *Curr Opin Neurobiol*. doi:10.1016/j.conb.2015.02.001

Atkinson PJ, Huarcaya Najarro E, Sayyid ZN, Cheng AG. 2015. Sensory hair cell development and regeneration: similarities and differences. *Development* **142**:1561–71. doi:10.1242/dev.114926

Barolo S, Castro B, Posakony JW. 2004. New Drosophila transgenic reporters: insulated P-element vectors expressing fast-maturing RFP. *Biotechniques* **36**:436–40, 442. doi:10.2144/04363ST03

Boekhoff-Falk G. 2005. Hearing inDrosophila: Development of Johnston's organ and emerging parallels to vertebrate ear development. *Dev Dyn* **232**:550–558. doi:10.1002/dvdy.20207

Boekhoff-Falk G, Eberl DF. 2014. The *Drosophila* auditory system. *Wiley Interdiscip Rev Dev Biol* **3**:179–191. doi:10.1002/wdev.128

Bramhall NF, Shi F, Arnold K, Hochedlinger K, Edge ASB. 2014. Lgr5-Positive Supporting Cells Generate New Hair Cells in the Postnatal Cochlea. *Stem Cell Reports* **2**:311–322. doi:10.1016/J.STEMCR.2014.01.008

Brignull HR, Raible DW, Stone JS. 2009. Feathers and fins: Non-mammalian models for hair cell regeneration. *Brain Res* **1277**:12–23. doi:10.1016/J.BRAINRES.2009.02.028

Bucks SA, Cox BC, Vlosich BA, Manning JP, Nguyen TB, Stone JS. 2017. Supporting cells remove and replace sensory receptor hair cells in a balance organ of adult mice. *Elife* **6**. doi:10.7554/eLife.18128

Corwin JT, Cotanche DA. 1988. Regeneration of sensory hair cells after acoustic trauma. *Science* **240**:1772–4.

Costa A, Sanchez-Guardado L, Juniat S, Gale JE, Daudet N, Henrique D. 2015. Generation of sensory hair cells by genetic programming with a combination of transcription factors. *Development* **142**:1948–59. doi:10.1242/dev.119149

Cox BC, Chai R, Lenoir A, Liu Z, Zhang L, Nguyen D-H, Chalasani K, Steigelman KA, Fang J, Rubel EW, Cheng AG, Zuo J. 2014. Spontaneous hair cell regeneration in the neonatal mouse cochlea in vivo. *Development* **141**:1599–1599. doi:10.1242/dev.109421

Eberl DF, Boekhoff-Falk G. 2007. Development of Johnston's organ in Drosophila. *Int J Dev Biol* **51**:679–687. doi:10.1387/ijdb.072364de

Fernández-Hernández I, Rhiner C, Moreno E. 2013. Adult Neurogenesis in Drosophila. *Cell Rep* **3**:1857–1865. doi:10.1016/j.celrep.2013.05.034

Fernández-Hernández I, Scheenaard E, Pollarolo G, Gonzalez C. 2016. The translational relevance of *Drosophila* in drug discovery. *EMBO Rep* **17**:471–472. doi:10.15252/embr.201642080

Forge A, Li L, Corwin JT, Nevill G. 1993. Ultrastructural evidence for hair cell regeneration in the mammalian inner ear. *Science* **259**:1616–9. doi:10.1126/science.8456284

Geleoc GSG, Holt JR. 2014. Sound Strategies for Hearing Restoration. *Science (80-)* **344**:1241062–1241062. doi:10.1126/science.1241062

Golub JS, Tong L, Ngyuen TB, Hume CR, Palmiter RD, Rubel EW, Stone JS. 2012. Hair cell replacement in adult mouse utricles after targeted ablation of hair cells with diphtheria toxin. *J Neurosci* **32**:15093–105. doi:10.1523/JNEUROSCI.1709-12.2012

Gong Z, Son W, Chung YD, Kim J, Shin DW, McClung CA, Lee Y, Lee HW, Chang D-J, Kaang B-K, Cho H, Oh U, Hirsh J, Kernan MJ, Kim C. 2004. Two interdependent TRPV channel subunits, inactive and Nanchung, mediate hearing in Drosophila. *J Neurosci* **24**:9059–66. doi:10.1523/JNEUROSCI.1645-04.2004

Inagaki HK, Kamikouchi A, Ito K. 2010. Methods for quantifying simple gravity sensing in Drosophila melanogaster. *Nat Protoc* **5**:20–25. doi:10.1038/nprot.2009.196

Ishikawa Y, Kamikouchi A. 2016. Auditory system of fruit fl ies **338**:1–8. doi:10.1016/j.heares.2015.10.017

Ishikawa Y, Okamoto N, Nakamura M, Kim H, Kamikouchi A. 2017. Anatomic and Physiologic Heterogeneity of Subgroup-A Auditory Sensory Neurons in Fruit Flies. *Front Neural Circuits* **11**:1–21. doi:10.3389/fncir.2017.00046

Kamikouchi A, Inagaki HK, Effertz T, Hendrich O, Fiala A, Göpfert MC, Ito K. 2009. The neural basis of Drosophila gravity-sensing and hearing. *Nature* **458**:165–171. doi:10.1038/nature07810

Kamikouchi A, Shimada T, Ito KEI. 2006. Comprehensive Classification of the Auditory Sensory Projections in the Brain of the Fruit Fly Drosophila melanogaster **356**:317–356. doi:10.1002/cne

Kawamoto K, Izumikawa M, Beyer LA, Atkin GM, Raphael Y. 2009. Spontaneous hair cell regeneration in the mouse utricle following gentamicin ototoxicity. *Hear Res* **247**:17–26. doi:10.1016/J.HEARES.2008.08.010

Kelley MW, Talreja DR, Corwin JT. 1995. Replacement of hair cells after laser microbeam irradiation in cultured organs of corti from embryonic and neonatal mice. *J Neurosci* **15**:3013–26. doi:10.1523/JNEUROSCI.15-04-03013.1995

Kil J, Warchol ME, Corwin JT. 1997. Cell death, cell proliferation, and estimates of hair cell life spans in the vestibular organs of chicks. *Hear Res*. doi:10.1016/S0378-5955(97)00166-4

Kniss JS, Jiang L, Piotrowski T. 2016. Insights into sensory hair cell regeneration from the zebrafish lateral line. *Curr Opin Genet Dev* **40**:32–40. doi:10.1016/j.gde.2016.05.012

Koehler KR, Mikosz AM, Molosh AI, Patel D, Hashino E. 2013. Generation of inner ear sensory epithelia from pluripotent stem cells in 3D culture. *Nature* **500**:217–221. doi:10.1038/nature12298

Koehler KR, Nie J, Longworth-Mills E, Liu X-P, Lee J, Holt JR, Hashino E. 2017. Generation of inner ear organoids containing functional hair cells from human pluripotent stem cells. *Nat Biotechnol* **35**:583–589. doi:10.1038/nbt.3840

Kwon Y, Shen WL, Shim H-S, Montell C. 2010. Fine thermotactic discrimination between the optimal and slightly cooler temperatures via a TRPV channel in chordotonal neurons. *J Neurosci* **30**:10465–71. doi:10.1523/JNEUROSCI.1631-10.2010

Lai JS, Lo S, Dickson BJ, Chiang A. 2012. Auditory circuit in the Drosophila brain **109**. doi:10.1073/pnas.1117307109

Landegger LD, Dilwali S, Stankovic KM. 2017. Neonatal Murine Cochlear Explant Technique as an In Vitro Screening Tool in Hearing Research. *J Vis Exp*. doi:10.3791/55704

Lee T, Luo L. 1999. Mosaic Analysis with a Repressible Cell Marker for Studies of Gene Function in Neuronal Morphogenesis. *Neuron* **22**:451–461. doi:10.1016/S0896-6273(00)80701-1

Li T, Bellen HJ, Groves AK. 2018. Using Drosophila to study mechanisms of hereditary hearing loss. *Dis Model Mech* **11**:dmm031492. doi:10.1242/dmm.031492

Marshall OJ, Brand AH. 2017. Chromatin state changes during neural development revealed by in vivo cell-type specific profiling. *Nat Commun* **8**:2271. doi:10.1038/s41467-017-02385-4

Marshall OJ, Southall TD, Cheetham SW, Brand AH. 2016. Cell-type-specific profiling of protein–DNA interactions without cell isolation using targeted DamID with next-generation sequencing. *Nat Protoc* **11**:1586–1598. doi:10.1038/nprot.2016.084

Matsuo E, Seki H, Asai T, Morimoto T, Miyakawa H, Ito K, Kamikouchi A. 2016. Organization of projection neurons and local neurons of the primary auditory center in the fruit fly *Drosophila melanogaster*. *J*

Comp Neurol **524**:1099–1164. doi:10.1002/cne.23955

Müller U, Barr-Gillespie PG. 2015. New treatment options for hearing loss. *Nat Rev Drug Discov* **14**:346–365. doi:10.1038/nrd4533

Ohlstein B, Spradling A. 2006. The adult Drosophila posterior midgut is maintained by pluripotent stem cells. *Nature* **439**:470–474. doi:10.1038/nature04333

Pfeiffer BD, Ngo TTB, Hibbard KL, Murphy C, Jenett A, Truman JW, Rubin GM. 2010. Refinement of tools for targeted gene expression in Drosophila. *Genetics* **186**:735–755. doi:10.1534/genetics.110.119917

Post Y, Clevers H. 2019. Perspective Defining Adult Stem Cell Function at Its Simplest : The Ability to Replace Lost Cells through Mitosis. *Stem Cell* **25**:174–183. doi:10.1016/j.stem.2019.07.002

Ryals BM, Dent ML, Dooling RJ. 2013. Return of function after hair cell regeneration. *Hear Res* **297**:113–120. doi:10.1016/j.heares.2012.11.019

Ryals BM, Rubel EW. 1988. Hair cell regeneration after acoustic trauma in adult Coturnix quail. *Science* **240**:1774–6.

Scrucca L, Fop M, Murphy TB, Raftery AE. 2016. mclust 5: Clustering, Classification and Density Estimation Using Gaussian Finite Mixture Models. *R J* **8**:289–317.

Shearin HK, MacDonald IS, Spector LP, Steven Stowers R. 2014. Hexameric GFP and mCherry reporters for the Drosophila GAL4, Q, and LexA transcription systems. *Genetics* **196**:951–960. doi:10.1534/genetics.113.161141

Singh AP, Das RN, Rao G, Aggarwal A, Diegelmann S, Evers JF, Karandikar H, Landgraf M, Rodrigues V, VijayRaghavan K. 2013. Sensory Neuron-Derived Eph Regulates Glomerular Arbors and Modulatory Function of a Central Serotonergic Neuron. *PLoS Genet* **9**:e1003452. doi:10.1371/journal.pgen.1003452

Southall TD, Gold KS, Egger B, Davidson CM, Caygill EE, Marshall OJ, Brand AH. 2013. Cell-type-specific profiling of gene expression and chromatin binding without cell isolation: Assaying RNA pol II occupancy in neural stem cells. *Dev Cell* **26**:101–112. doi:10.1016/j.devcel.2013.05.020

Stone JS, Cotanche DA. 2007. Hair cell regeneration in the avian auditory epithelium. *Int J Dev Biol* **51**:633–647. doi:10.1387/ijdb.072408js

Sun Y, Liu L, Ben-Shahar Y, Jacobs JS, Eberl DF, Welsh MJ. 2009. TRPA channels distinguish gravity sensing from hearing in Johnston's organ. *Proc Natl Acad Sci U S A* **106**:13606–11. doi:10.1073/pnas.0906377106

Vaughan AG, Zhou C, Manoli DS, Baker BS. 2014. Neural Pathways for the Detection and Discrimination of

Conspecific Song in D . melanogaster. *Curr Biol* **24**:1039–1049. doi:10.1016/j.cub.2014.03.048

Wang VY, Hassan BA, Bellen HJ, Zoghbi HY. 2002. Drosophila atonal Fully Rescues the Phenotype of Math1 Null Mice: New Functions Evolve in New Cellular Contexts. *Curr Biol* **12**:1611–1616. doi:10.1016/S0960-9822(02)01144-2

Warchol M, Lambert P, Goldstein B, Forge A, Corwin J. 1993. Regenerative proliferation in inner ear sensory epithelia from adult guinea pigs and humans. *Science (80-)* **259**:1619–1622. doi:10.1126/science.8456285

White PM, Doetzlhofer A, Lee YS, Groves AK, Segil N. 2006. Mammalian cochlear supporting cells can divide and trans-differentiate into hair cells. *Nature* **441**:984–987. doi:10.1038/nature04849

Williams J., Holder N. 2000. Cell turnover in neuromasts of zebrafish larvae. *Hear Res* **143**:171–181. doi:10.1016/S0378-5955(00)00039-3

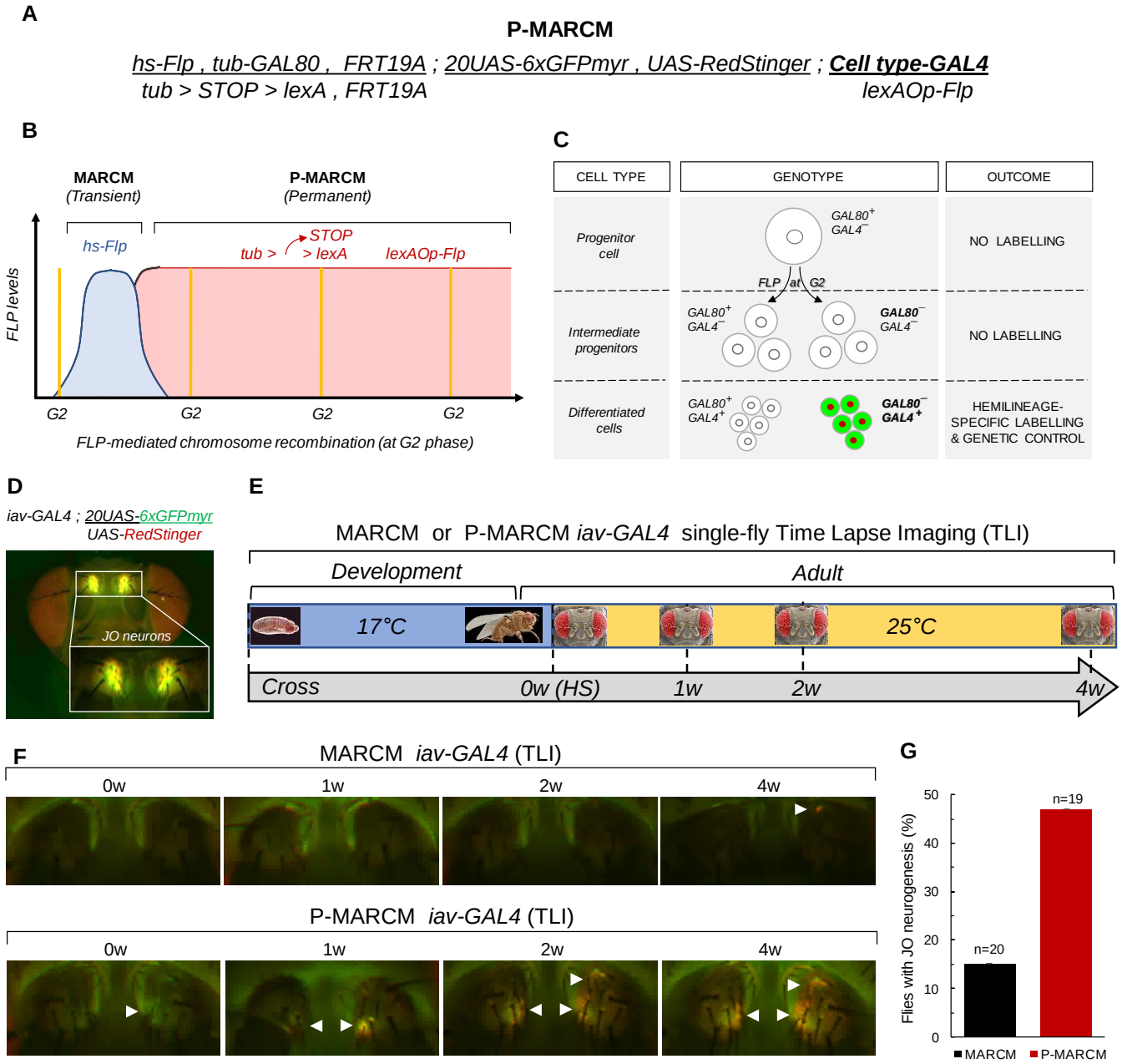

Figure 1. P-MARCM captures Johnston's Organ (JO) neurogenesis in adult *Drosophila*

(A) P-MARCM system to label and genetically manipulate adult-born cells in *Drosophila* in a cell type-specific manner.

(B) P-MARCM becomes permanently active to mediate mitotic chromosome recombination by switching a transient pulse of Flippase (Flp) into a constitutive one in Heat Shock (HS)-activated cells.

(C) P-MARCM labels only adult-born cells of interest in a lineage by introducing cell type-specific *GAL4* lines (*iav-GAL4* in these experiments). Enginereed nuclear-red and membrane-green fluorescent reporters allow quantification and cellular morphology assesment with no antibodies.

(D) .*iav-GAL4* in conjunction with engineered fluorescent reporters allows JO neurogenesis assessment in live flies by Time-Lapse Imaging (TLI).

(E) JO neurogenesis can be ns are detected in live flies

(F) Experimental strategy to capture JO adult neurogenesis by MARCM or P-MARCM *iav-GAL4*: flies were kept at 17C during development to minimize leaky activation; 2-5 days-old flies were heat shock-activated and antennae of individual flies imaged over 4 weeks by fluorescent microscopy.

(F-G) Unlike regular MARCM, P-MARCM identifies JO neurogenesis in *Drosophila* antenae over time at a higher frequency and extent.

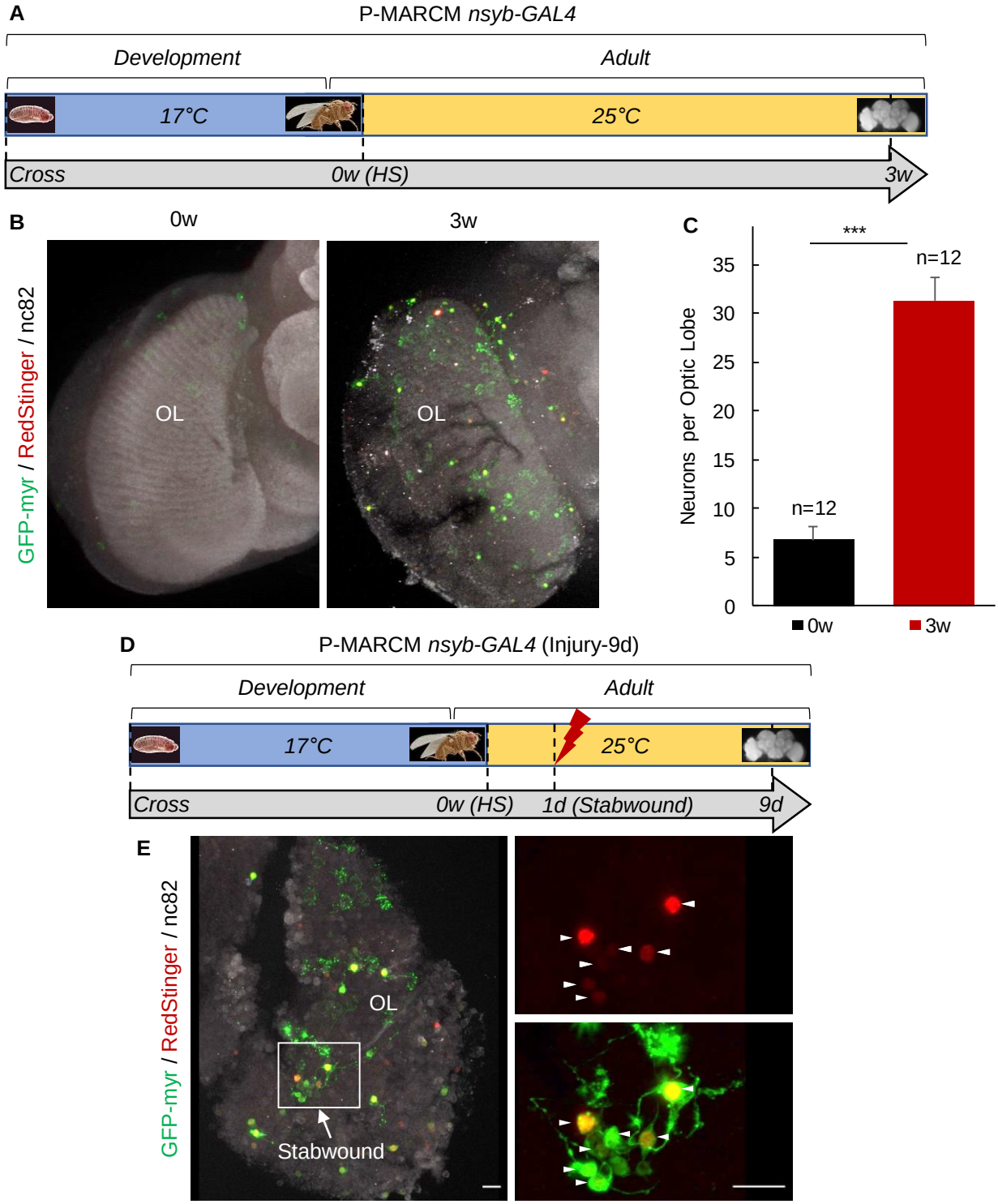

Figure supplement 1. P-MARCM captures previously-reported adult neurogenesis and regeneration in the *Drosophila* optic lobes (OL)

(A) Experimental strategy to capture adult neurogenesis with P-MARCM *nsyb-GAL4*. Flies 2-5 days–old were Heat-Shocked (HS) to activate the P-MARCM system and brains were dissected 3 weeks (3w) after.

(B) Adult-born neurons in the optic lobes (OL) are specifically labeled by P-MARCM with *nsyb-GAL4* line over 3 weeks after HS.

(C) Amount of adult-born neurons in OL at 3 weeks is significantly higher than background levels in the system ($p<0.001$). Error bars represent SEM.

(D) Experimental strategy to capture injury-induced neuronal regeneration in OL with P-MARCM *nsyb-GAL4*. Flies 2-5 days–old were Heat-Shocked (HS) to activate the P-MARCM system. Stabwound was applied on left OL by a fine needle 1 day after HS and scanned 9 days later.

(E) Regenerated neurons in the OL (arrowheads) are specifically labeled by P-MARCM with *nsyb-GAL4* line 9 days after stabwound. Scale bar: 10 μm.

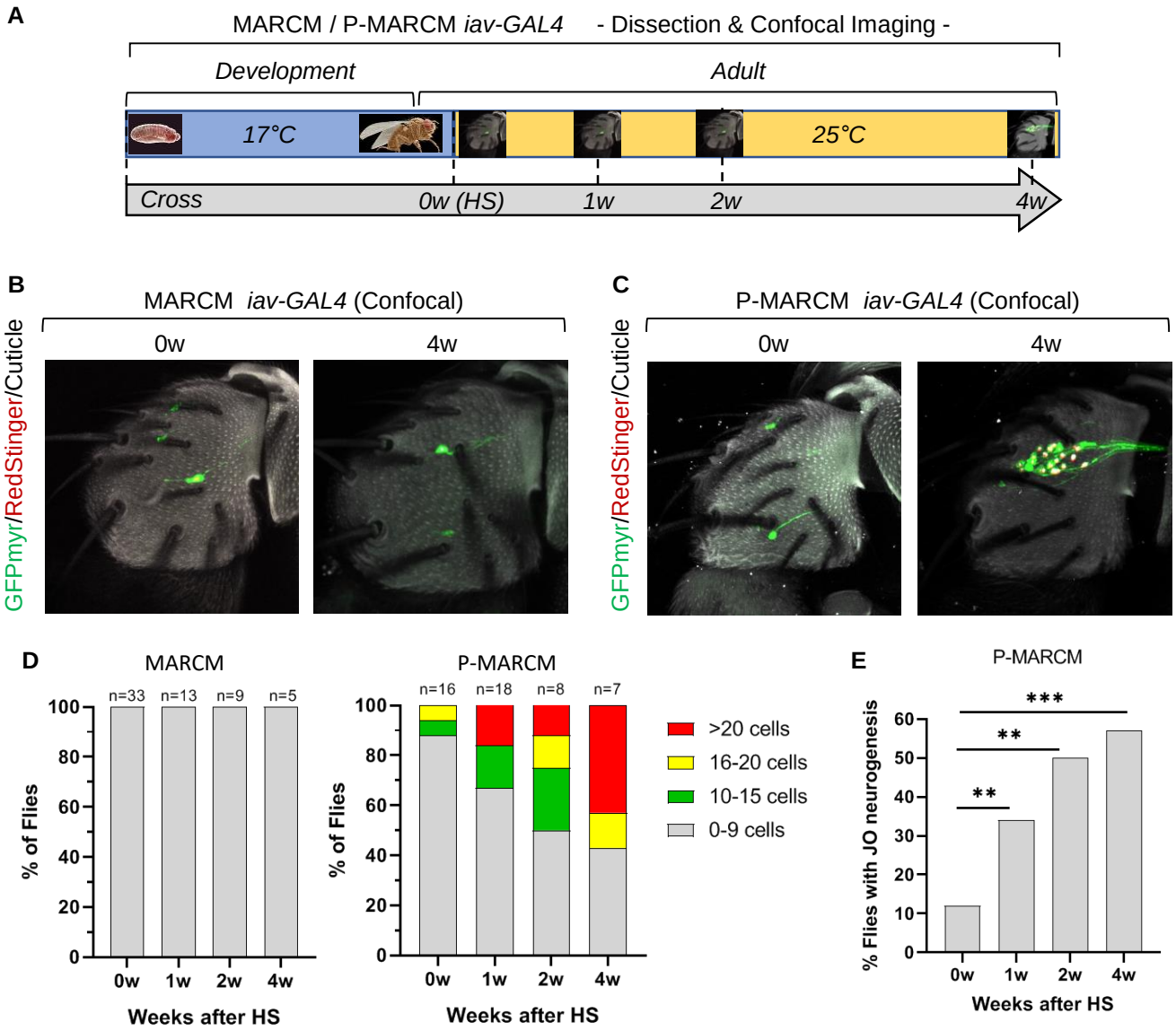

Figure 2. P-MARCM *iav-GAL4* reports on previously undetected levels of adult JO neurogenesis.

(A) Experimental strategy to capture adult JO neurogenesis by MARCM and P-MARCM *iav-GAL4*. Flies 2-5 days–old were Heat-Shocked (HS) to activate the MARCM or P-MARCM system and antennae were dissected at different time points over 4 weeks for quantification.
(B) Transient MARCM *iav-GAL4* does not capture JO neurogenesis.
(C) P-MARCM *iav-GAL4* captures adult-born JO neurons.
(D) Accumulation of JO neurons is detected in antennae of P-MARCM, but not MARCM flies.
(E) Frequency of flies with JO neurogenesis increases over time.

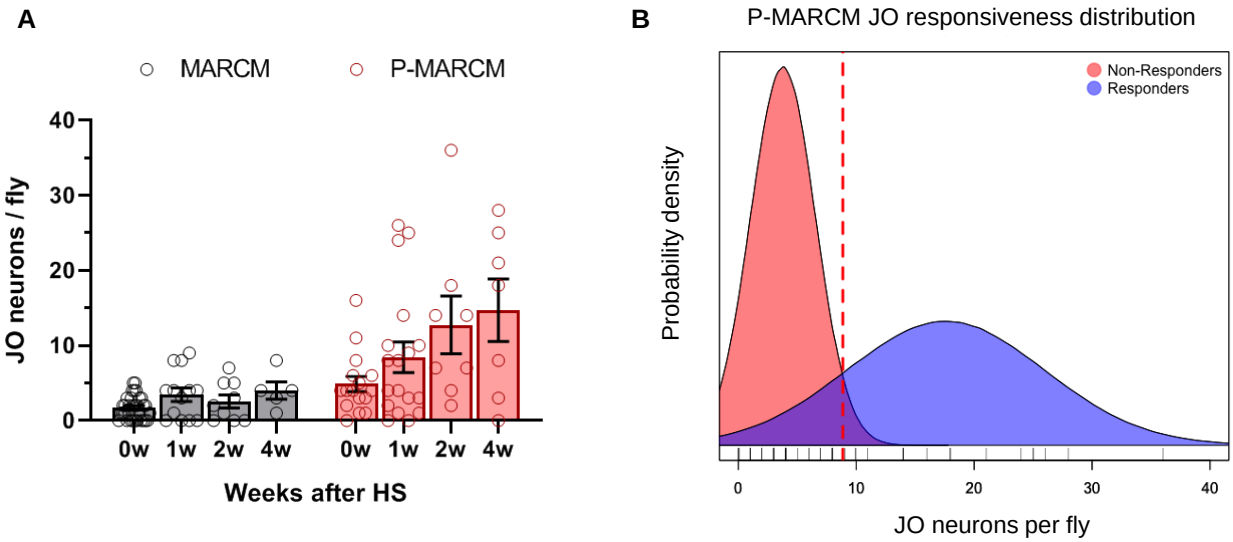

Figure supplement 2. JO neurogenesis detection and distribution

(A) Oppositve to MARCM, P-MARCM captured JO neurogenesis over time beyond system background levels in a binomial distribution.

(B) (B) Gaussian mixture model classifies flies into ‘Responders’/’Non-respponders’ (i.e. JO neurogenesis present/absent)

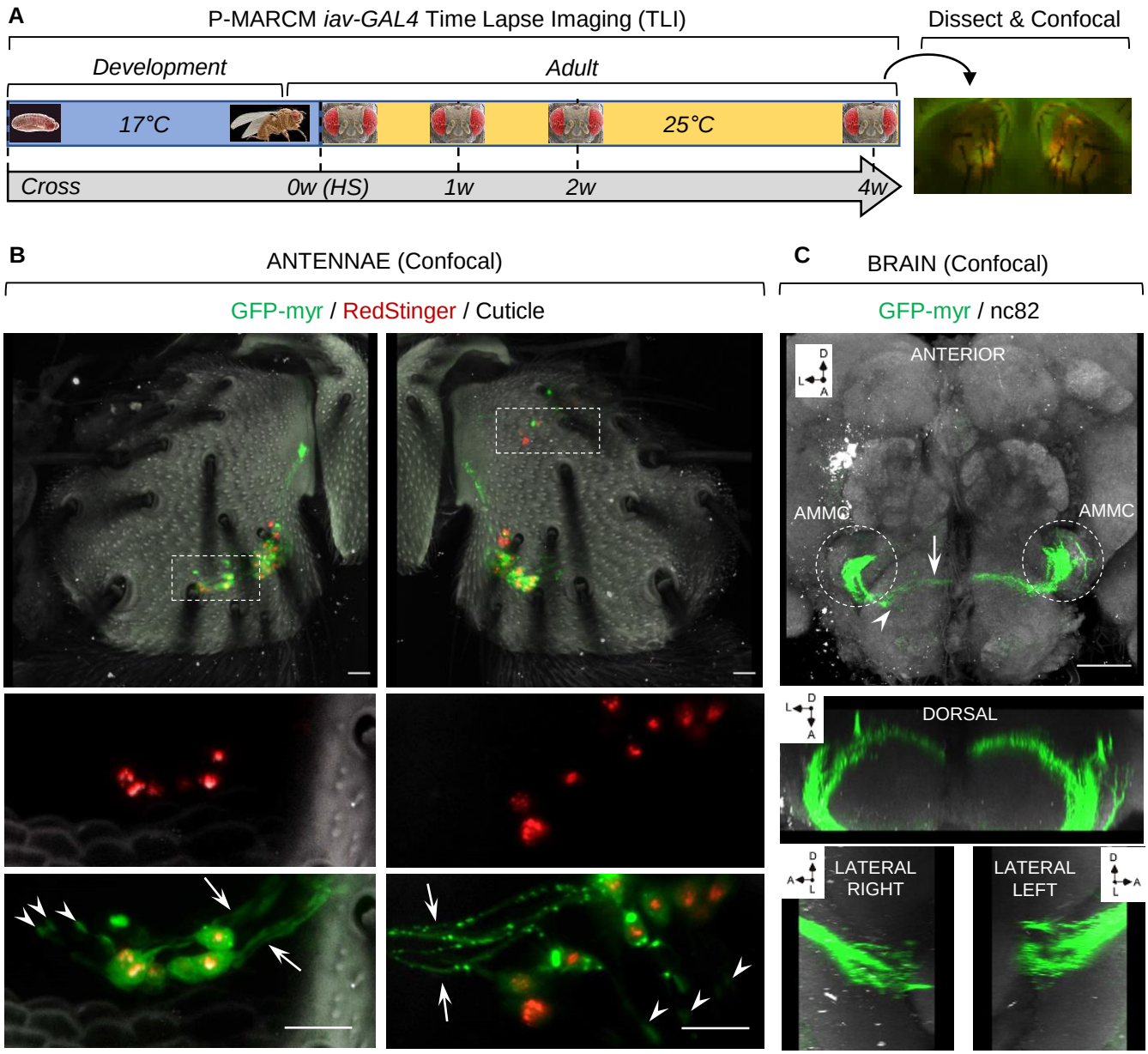

Figure 3. Adult-born JO neurons acquire mechanosensory features and target brain circuitry.

(A) P-MARCM *iav-GAL4* flies with adult JO neurogenesis detected by Time Lapse Imaging (see Figure 1F) were dissected for detailed cellular analysis by confocal microscopy.

(B) Adult-born JO neurons develop cilia (arrowhead), express the essential mechanotransducer channel *iav* and project axons to the brain (arrows). Scale bar: 10 μm

(C) Axons from adult-born JO neurons target the brain at the Antennal Mechanosensory and Motor Center (AMMC) in the auditory (arrowhead) and vestibular (arrow) pattern. Scale bar: 50 μm. A: Anterior D: Dorsal L: Lateral

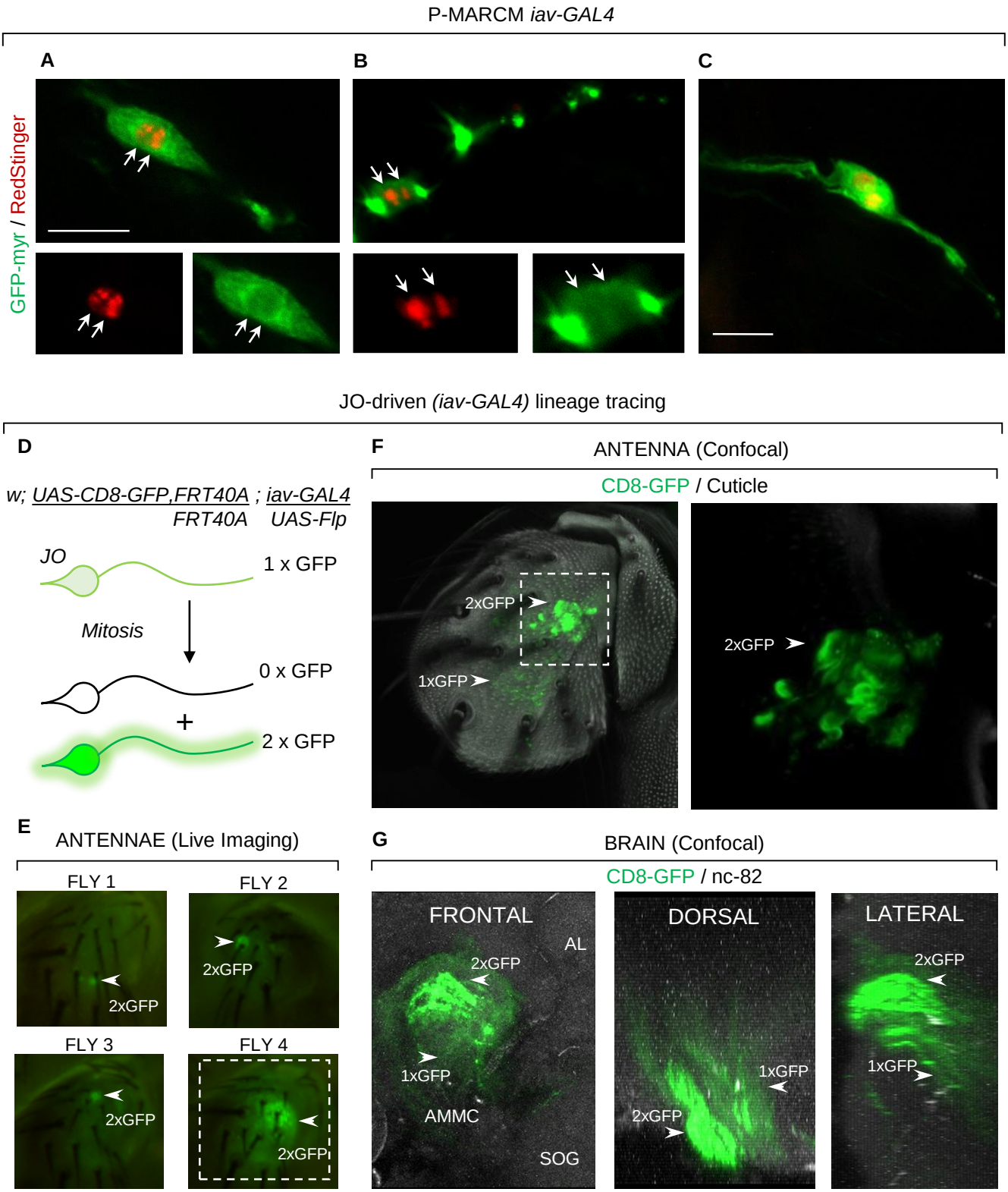

Figure 4. Adult JO neurons undergoe self-division

--- Figure legend on next page ---

Figure 4. Adult JO neurons undergo self-division

(A-C) P-MARCM *iav-GAL4* captures JO neurons with split DNA (A,B) and tightly-closed labelled ones (C), suggesting mitotic acitivity.

(D) A lineage tracing system to assess JO self-division: *iav-GAL4* drives constitutive expression of membrane-tethered GFP and FLP recombinase in virtually all JO neurons. Upon mitosis, one JO becomes homozygous for GFP, thus reporting on self-division.

(E) JO self-proliferation is detected by live fluorescent microscopy in flies at 2 weeks after eclossion (arrowheads). Fly4 is shown in panel (F).

(F) Self-replicated JO neuron are detected in the antennae by confocal microscopy

(G) Axons expressing two copies of GFP appear in the brain, suggesting entire replication of JO neuron, from cilia through terminal connections. Scale bars: 10 μm.

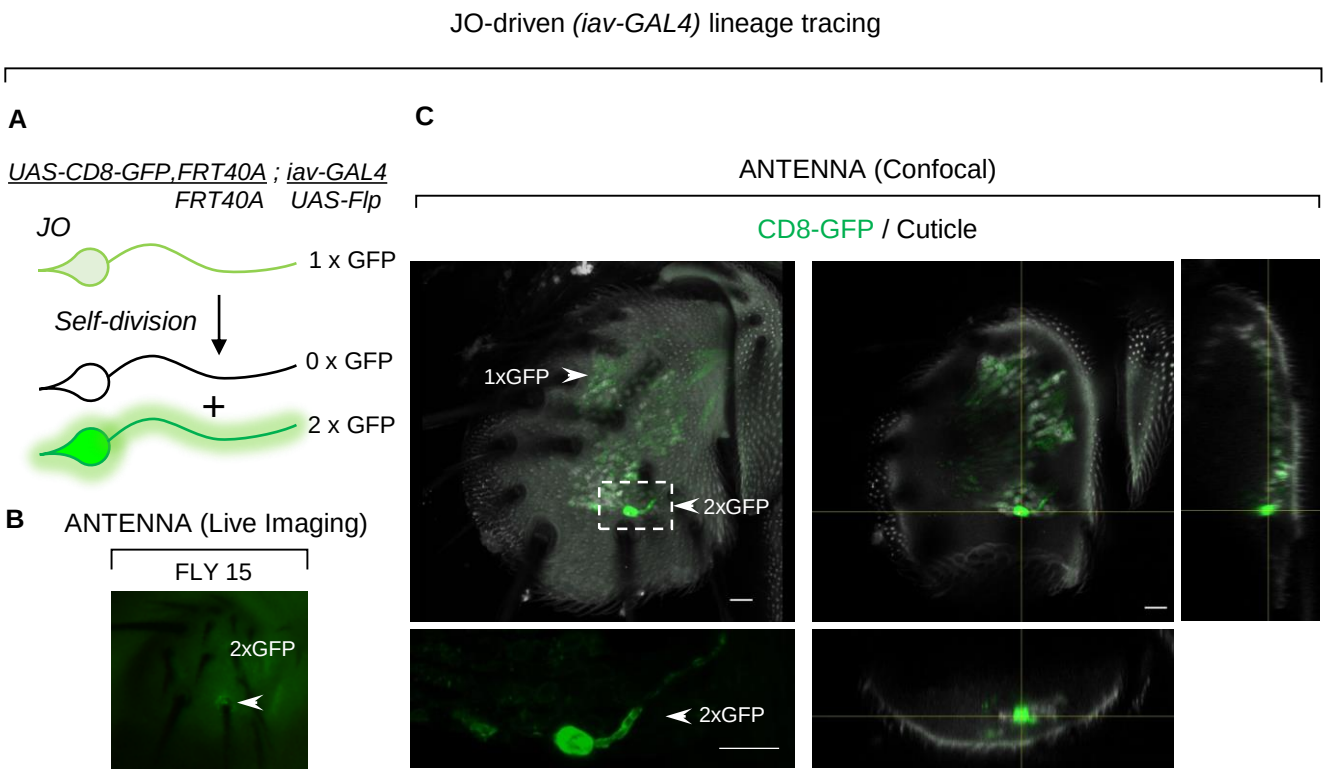

Figure supplement 3. Self-dividing JO neurons are captured at single-cell resolution *in vivo*.

(A) *.iav-GAL4*-driven lineage tracing system to assess JO self-replicaton.
(B) A single JO neuron expressing 2xGFP detected by live fluorescent microscopy.
(C) Confocal microscopy confirms proliferation of a single neuron on the anterior part of the antena. Scale bar: 10μm.

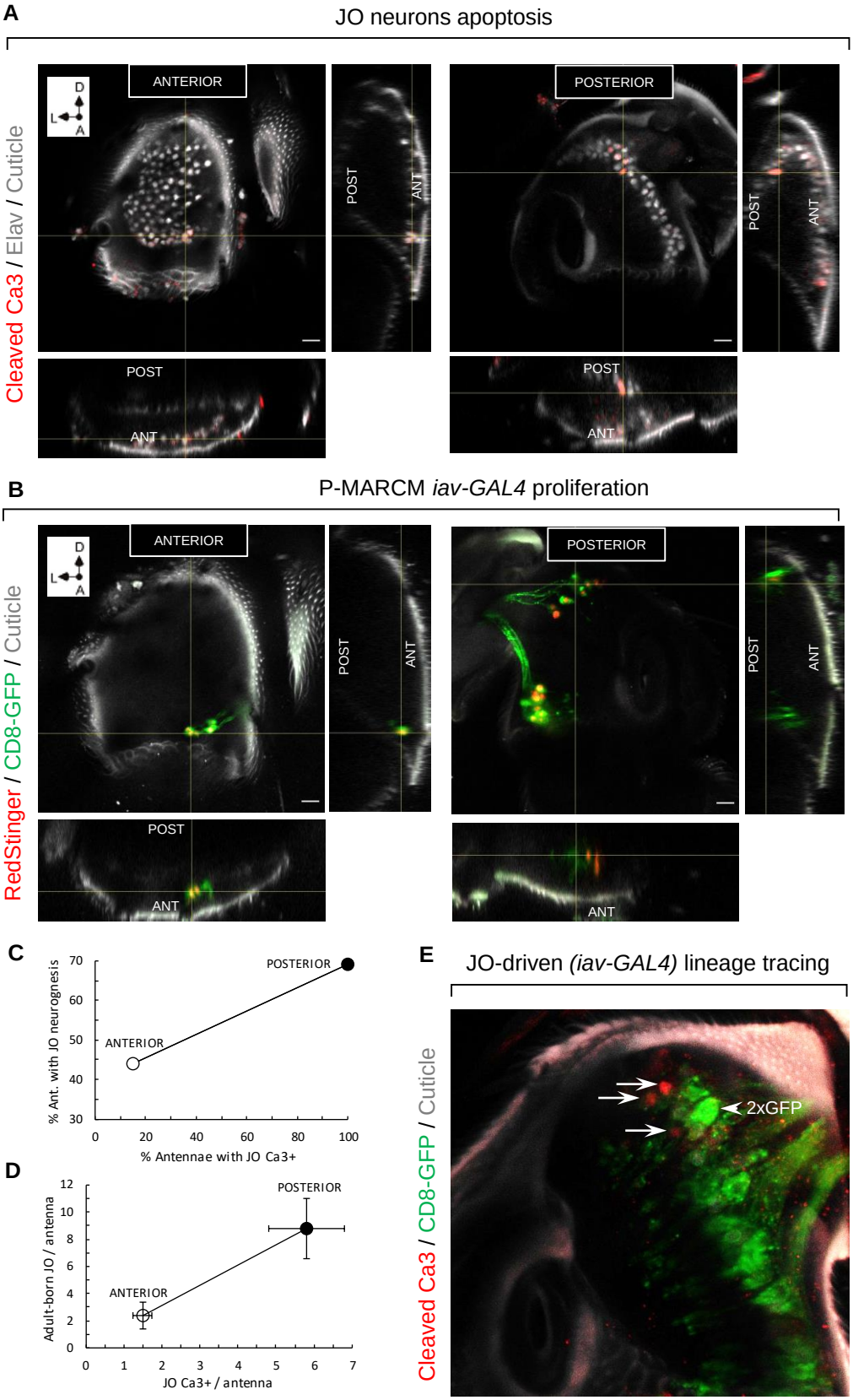

Figure 5. JO apoptosis and neurogenesis are spatially correlated.

(A) Apoptotic JO neurons (Cleaved Ca3/Elav) are detected anteriorly and posteriorly in the JO array.
(B) P-MARCM *iav-GAL4* detects JO neurogenesis in posterior and anterior regions of the JO array.
(C) Frequency of apoptosis correlates with frequency of adult JO neurogenesis detected by P-MARCM.
(D) Extent of apoptotic JO correlates with extent of adult-born JO detected by P-MARCM. Data shown is from two separate experiments.
(E) JO self-división (arrowhead) occurs nearby apoptotic JO neurons (arrows). Scale bars: 10μm.